The Radial Transport of Energetic Solar Flare Particles From 1 to 6 AU

DOUGLAS C. HAMILTON

Enrico Fermi Institute and Department of Physics, University of Chicago, Chicago, Illinois 60637

The Pioneer 10 and 11 missions to Jupiter and beyond have provided the first opportunity to observe solar flare accelerated particles at distances of several astronomical units from the sun. The intensity-time profiles out to at least 6 AU are consistent with mainly diffusive interplanetary propagation. No obvious effects of a free escape boundary have been observed, which implies that the outer boundary of the diffusion region is beyond 10 AU. Four solar particle events are discussed in detail. These are events during which azimuthal propagation and corotation effects played a relatively minor role at least until the time of maximum intensity. Their intensity-time profiles, which were observed simultaneously at two or three well-separated radial positions (with Imp 6 or Imp 8 at 1 AU and with Pioneer 10 and/or Pioneer 11 at 2.7–6.1 AU), are used to study the radial transport of energetic particles in interplanetary space. The events are interpreted in terms of a spherically symmetric propagation model (which is also appropriate within the flux tube from the coronal release site even if $K_{\parallel} \gg K_{\perp}$) which includes the effects of diffusion, convection, and adiabatic deceleration and which assumes that the particles are impulsively injected at the sun. If the effective radial diffusion coefficient is assumed to have the form $K_r = K_r(1\text{ AU})(r/r_e)^b$, the average value of the radial index b is found to be 0.4 ± 0.2. The average radial diffusion coefficient at 1 AU for 11- to 20-MeV protons is $K_r(1\text{ AU}) = (1.7 \pm 0.2) \times 10^{21}$ cm^2/s; for 30- to 67-MeV protons, $K_r(1\text{ AU}) = (2.9 \pm 0.2) \times 10^{21}$ cm^2/s; and for 1- to 2-MeV electrons, $K_r(1\text{ AU}) = (4\text{–}9) \times 10^{21}$ cm^2/s, all for the period 1972–1974. The corresponding radial mean free paths at 1 AU are $\lambda_r(1\text{ AU}) = 0.065 \pm 0.010$ AU independent of energy for protons from 11 to 67 MeV and $\lambda_r(1\text{ AU}) = 0.03\text{–}0.06$ AU for the 1- to 2-MeV electrons. The measured solar wind speeds are used to estimate the solar connection longitude of each spacecraft in order to interpret better the observed intensity-time profiles in terms of radial propagation and corotation. It is found that when the calculated solar connection longitude remains nearly constant during an event (a 'dwell' region), a period during which corotation effects are minimized, the model intensity-time prediction tends to agree with that observed even in the decay phase of the event. The maximum intensity is found to decrease with radial distance as r^{-3} to r^{-4}, which is consistent with the cross-sectional area of the flux tube containing the particles increasing as r^2 (or somewhat faster than r^2 in dwell regions).

INTRODUCTION

Ever since it was discovered that many aspects of the intensity-time profiles of energetic solar flare particles were explained by assuming a diffusive mode of propagation in interplanetary space [*Meyer et al.*, 1956], the details of the process, and their relationship to the properties of the interplanetary medium, have been under investigation. It soon became apparent that there is a persistent magnetic field in interplanetary space which conforms, on the average, to an Archimedean spiral and that charged particle propagation is much easier along than across the field. So the initial simplified picture of isotropic diffusion characterized by a scalar diffusion coefficient K was modified to reflect its more complicated tensor nature with $K_{\parallel}$, the magnitude of K_{ij} parallel to the average magnetic field direction, being much larger than $K_{\perp}$, the magnitude perpendicular to that direction.

Parker [1965] generalized the theory of cosmic ray transport to include the effects of convection and adiabatic energy loss in the expanding solar wind with the resulting equation for the differential number density $U(x_i, T, t)$

$$\frac{\partial U}{\partial t} + \frac{\partial}{\partial x_i}(V_i U) - \frac{\partial}{\partial x_i}\left(K_{ij}\frac{\partial U}{\partial x_j}\right) + \frac{\partial}{\partial T}\left(U\frac{dT}{dt}\right) = 0 \quad (1)$$

where the second, third, and fourth terms represent the effects of convection, diffusion, and energy change, respectively. The rate of energy loss is given by

$$\frac{1}{T}\frac{dT}{dt} = -\frac{\alpha}{3}\frac{\partial V_i}{\partial x_i}$$

where V_i is the solar wind velocity, t is time, T is the kinetic energy of the particle, and $\alpha = (T + 2m_0c^2)/(T + m_0c^2)$.

Copyright © 1977 by the American Geophysical Union.

Paper number 7A0212.

The attempt to determine the value of K_{ij} has proceeded along two lines. One approach has been to relate theoretically the magnitude of K_{ij} to the measured power spectrum of irregularities in the interplanetary magnetic field (IMF) (see *Jokipii* [1971] and *Völk* [1975] and references therein). The other approach has been a phenomenological one, interpreting time or spatial variations of energetic charged particle intensity (either galactic or solar) in terms of (1) or a modification of it. In this report we take the second course with the intention of better specifying the radial dependence of K_{ij} using simultaneous observations of solar flare particle events at 1 AU made with instruments on the earth satellites Imp 6 and 8 and at radial distances of 2.7–6.1 AU from the sun with instruments on Pioneer 10 and 11.

There have been a number of attempts to determine experimentally the radial dependence of K_{ij}, several using observations of solar particle events (SPE). Many of them are summarized in Table 1. In most cases a power law form for the radial dependence was assumed, $|K_{ij}| \propto r^b$, so the value found for the radial index b has been listed. If it is not otherwise specified, b is the radial index for an assumed isotropic diffusion coefficient (or equivalently for radial transport, the radial diffusion coefficient K_r).

In order to compare meaningfully the various results in Table 1 it is important to note the type of measurement on which each is based. Those results which are derived from the value of t_m (the time to maximum intensity) of an SPE depend mainly on K_{ij} between the sun and the point of observation. Those which are derived from fitting the intensity profile into the decay phase as well are also affected by K_{ij} at radii greater than the radius of the observation point. Inside 1 AU, $K_{\parallel}$ differs little from K_r, so the result of *Sari* [1973] can be compared directly with the others. However, if $K_{\parallel} \gg K_{\perp}$, K_r and

TABLE 1. Summary of Experimental Investigations of the Radial Dependence of K_{ij}

Investigator	Model Used	Data Used	Results
Hofmann and Winckler [1963]	isotropic diffusion	intensity-time profile of July 20, 1961, SPE at earth	$b \gtrsim 3$
Parker [1965]	isotropic and anisotropic diffusion	decay phase of some SPE's at earth	$b = 0.0$–0.5 if K_{ij} isotropic; $b = 2.0$–2.5 if $K_{\parallel} >> K_{\perp}$
Krimigis [1965]	isotropic diffusion	intensity-time profiles of three SPE's at earth	$b = \frac{3}{2}$–1
Feit [1969]	anisotropic diffusion	intensity-time profiles of five SPE's at earth	$b = 0.6$–1.0 for K_r
Lupton and Stone [1973]	anisotropic diffusion, convection, and adiabatic deceleration	intensity-time profiles of three SPE's at earth	found $b = 0$ preferable to $b = 1$ for K_r
Webb et al. [1973]	isotropic diffusion, convection, and adiabatic deceleration	time to maximum intensity for three SPE's at earth plus measured interplanetary plasma field parameters	$b \sim -3$–0 depending on assumptions made about the magnetic field fluctuations
Sari [1973]	anisotropic diffusion	power spectra of IMF between 1.0 and 0.8 AU plus time to maximum at earth of 70-MeV solar flare protons plus measurement of gradient of GCR's near 1 AU and estimate of total modulation factor	$b < -1$ for $K_{\parallel}$ inside of 1 AU
Cummings et al. [1973]	anisotropic diffusion and convection	power spectrum of IMF at earth plus estimate of the modulation factor for electrons	$b \lesssim 1.2$
Hamilton [1975]	isotropic diffusion, convection, and adiabatic deceleration	time to maximum intensity of Nov. 3, 1973, SPE at 1.0 and 2.7 AU	$0 < b < 1$
Countee and Lanzerotti [1976]	isotropic diffusion, convection, and adiabatic deceleration	intensity-time profiles of two SPE's at earth	found $b = 1$ preferable to $b = 0$
McCarthy and O'Gallagher [1976]	anisotropic diffusion	anisotropy amplitude for 3- to 10-MeV protons at time of maximum intensity for 24 SPE's as function of radial distance from 1.0 to 4.7 AU	$b = 0.9 \pm 0.4$ for $K_{\parallel}$
This work	isotropic diffusion, convection, and adiabatic deceleration	time to maximum intensity for four SPE's measured at earth and simultaneously at distances of 2.7–6.1 AU	$b = 0.4 \pm 0.2$

$K_{\parallel}$ have greatly differing radial dependences beyond 1 AU. So the value of b deduced for $K_{\parallel}$ by *McCarthy and O'Gallagher* [1976] corresponds to $b \sim -0.5 \pm 0.4$ for K_r (assuming $K_r = K_{\parallel} \cos^2 \psi$, where ψ is the spiral angle), since $\cos^2 \psi \sim r^{-1.4}$ between 1 and 5 AU. Although there is considerable spread in the values of b found, over half the results lie between 0 and 1 (a feature implying that K_r increases with radial distance).

A limitation of the previous experimental studies is that, except for the work of *Hamilton* [1975] and *McCarthy and O'Gallagher* [1976], all the observations were made in a small radial range near earth. The measurements of McCarthy and O'Gallagher covered a large radial range but were made serially, so that their results may be subject to temporal effects. By utilizing simultaneous observations of individual solar particle events at widely separated radial distances we hope to avoid some of these problems.

This report presents observations of four SPE's for which both earth and Pioneer 10 or Pioneer 11 appear to be well connected by the interplanetary magnetic field to the flare site (or coronal release site). These events can justifiably be analyzed in terms of the radial transport equation. Once a functional form for the radial dependence of K_r is chosen (a power law dependence is assumed here), both its magnitude and radial variation can be determined from the relatively simple and straightforward measurement of t_m at two radial distances.

In addition, the radial dependence of the maximum flux and the rigidity dependence of the radial mean free path are discussed. Finally, the radial dependence of t_m for all nine 'prompt' SPE's observed at Pioneer 10 or 11 from 1972 to 1975 is discussed. This group includes five events which were prompt only at Pioneer 10 or 11 as well as the four events which were also prompt at earth.

The experimental results to be presented are restricted to protons with energies between 11 and 67 MeV and electrons with energies between 1 and 2 MeV. The propagation of lower-energy protons (~1 MeV or less) is complicated, and the intensity profiles are usually dominated by local conditions of the interplanetary medium or by the details of coronal injection [e.g., *Roelof and Krimigis*, 1973]. The intensity-time profiles of low-energy solar protons are rarely of the classical diffusive type.

INSTRUMENT DESCRIPTIONS

Data from University of Chicago charged particle telescopes on the deep space probes Pioneer 10 and Pioneer 11 and the earth satellites Imp 6 and Imp 8 have been utilized. Figure 1 presents schematic cross sections of the two types of instruments. The species and energy of the incident particles are determined by dE/dx versus residual E analysis. When the particle flux is high, only a random sample of the incident particles is pulse height analyzed, and the absolute flux is determined by normalizing to a counting rate which records all the particles stopping in a given detector. All four spacecraft are spinning. The spin planes of the Imp 6 and 8 instruments are parallel to the ecliptic, while those of the Pioneer 10 and 11 instruments are perpendicular to the ecliptic. Only spin-averaged fluxes are presented in this paper.

The background counting rates for these instruments are kept at a low level by using an anticoincidence cylinder around the detector stack. Minimization of the background rate is especially important, since we require a measurement of the

21562202, 1977, 16, Downloaded from https://agupubs.onlinelibrary.wiley.com/doi/10.1029/JA082i016p02157 by Utah State University, Wiley Online Library on [13/06/2025]. See the Terms and Conditions (https://onlinelibrary.wiley.com/terms-and-conditions) on Wiley Online Library for rules of use; OA articles are governed by the applicable Creative Commons License

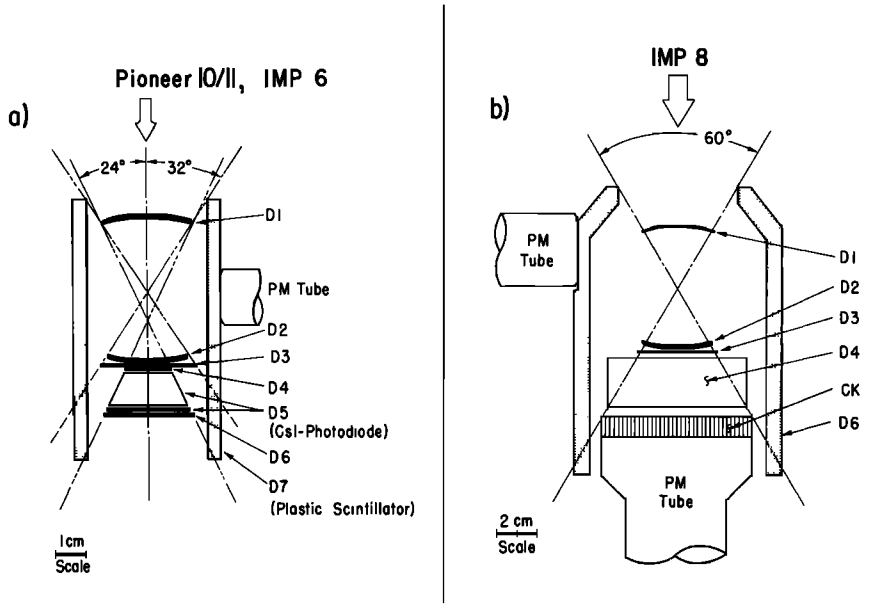

Fig. 1. Schematic cross sections of the University of Chicago charged particle telescopes on board Pioneer 10 and 11 and Imp 6 and 8. The solid shaded detectors are Si(Li). For Pioneer 10 and 11, detectors D1, D2, and D5 are pulse height analyzed. The geometrical factor is 1.3 cm² sr for particles stopping in D2 and 0.43 cm² sr for particles stopping in D5. For Imp 8, detectors D1 (or CK), D2, and D4 are pulse height analyzed. The geometrical factor is 2.05 cm² sr for all particles.

small residual flux of solar particles far from the sun. The 11- to 20-MeV protons discussed in this paper stop in the second silicon detector D2, and the 30- to 67-MeV protons stop in the CsI crystal (D5 for Pioneer 10 and 11 and Imp 6, D4 for Imp 8). The exact proton energy intervals for the four instruments are listed in Table 2. The full energy range of protons which stop in detector D4 in Imp 8 is 30–95 MeV; however, only the flux in the range 30–69 MeV was used for comparison with the analogous Pioneer 10 and 11 energy range. The 1- to 2-MeV electrons stop in detector D2 of both types of instrument.

The trajectories of Pioneer 10 and 11 are shown in Figure 2. The locations of the spacecraft at the times of the SPE's to be discussed are labeled by the day of year on which the parent flare occurred.

MODEL

For the simple case of a steady uniform solar wind with spherical symmetry and isotropic diffusion the general Fokker-Planck equation (1) reduces to

$$\frac{\partial U}{\partial t} + \frac{1}{r^2}\frac{\partial}{\partial r}\left(r^2 VU - r^2 K_r \frac{\partial U}{\partial r}\right) - \frac{2V}{3r}\frac{\partial}{\partial T}(\alpha T U) = 0 \quad (2)$$

where $U(r, T, t)$ is differential number density, r is the radial distance from the sun, T is kinetic energy, t is time, V is the solar wind speed, and K_r is the radial diffusion coefficient.

Following *Webb and Quenby* [1973], we have solved (2) numerically assuming a delta function injection of particles at the sun and an outer free escape boundary at $r = L$. In order to remove the explicit energy dependence in (2), so that the number of independent variables is reduced to two (r and t), we assumed that the number density energy spectrum could be expressed as a power law in T, $U = U_0 T^{-\gamma}$, where γ is the spectral index. We also assumed a power law dependence of K_r on r, writing $K_r = K_r(r_s)(r/r_s)^b$, independent of energy, where r_s is the solar radius and $K_r(r_s)$ is the value of K_r at $r = r_s$.

We found that a change of variables allowing logarithmic spacing in r increased the accuracy of the numerical solution for a fixed number of grid points (and therefore the amount of computing time) by giving a high density of grid points near the sun, where gradients are largest after an impulsive injection of particles. This change also made it possible to place the outer free escape boundary at a large distance from the sun (e.g., L = 20–50 AU) without requiring an inordinately large number of grid points.

TABLE 2. Proton Energy Intervals

	Pioneer 10	Pioneer 11	Imp 6	Imp 8
'11–20' MeV	10.4–19.6	10.5–19.5	10.6–19.8	11.2–20.0
'30–67' MeV	28.6–66.0	29.1–65.0	31.3–67.5	29.8–69.0

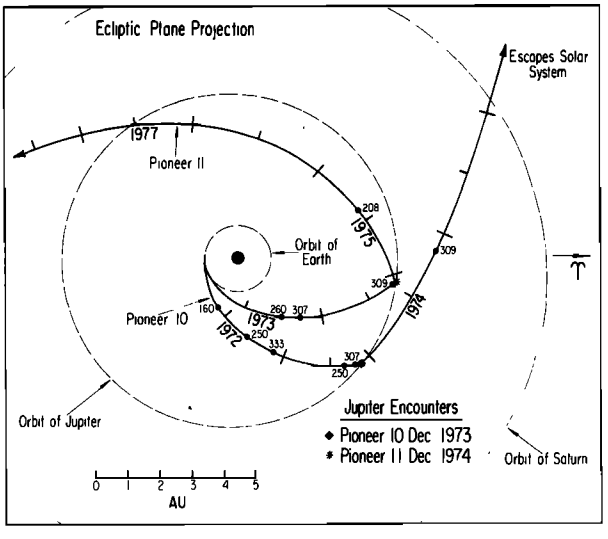

Fig. 2. Trajectories of Pioneer 10 and Pioneer 11. Solid circles indicate the positions of the spacecraft at the times of the various solar particle events and are labeled with the day of year on which the parent flare occurred.

21562202, 1977, 16, Downloaded from https://agupubs.onlinelibrary.wiley.com/doi/10.1029/JA082i016p02157 by Utah State University, Wiley Online Library on [13/06/2025]. See the Terms and Conditions (https://onlinelibrary.wiley.com/terms-and-conditions) on Wiley Online Library for rules of use; OA articles are governed by the applicable Creative Commons License

We define $q \equiv \ln (r/r_s)$ and $\tau \equiv K_r(r_s)t/r_s^2$, and (2) transforms to

$$\frac{\partial U}{\partial \tau} + e^{-q}\left[\frac{Vr_s}{K_r(r_s)} - (1+b)e^{q(b-1)}\right]\frac{\partial U}{\partial q} - e^{q(b-2)}\frac{\partial^2 U}{\partial q^2} + \frac{2Vr_s}{K_r(r_s)}e^{-q}\left[1 - \frac{\alpha}{3}(1-\gamma)\right] = 0 \quad (3)$$

This differential equation can then be written as a finite difference equation and solved numerically by using the Crank-Nicholson method. We did not find it necessary to change variables to include an approximate time dependence, as did *Webb and Quenby* [1973]. The boundary conditions used were $U = 0$ at $r = L$ for all t and $\partial U/\partial r = 0$ at $r = r_s$ (or $q = 0$) for $t > 0$. The radial streaming is given by

$$S_r = CVU - K_r\,\partial U/\partial r$$

where C is the Compton-Getting factor. For a totally reflecting sun the requirement is $S_r = 0$ at $r = r_s$, and the second boundary condition above approximates this closely, since for the range of parameters used the convective streaming is small in comparison with the diffusive streaming. In any case, several investigators have found that the choice between boundary conditions corresponding to an absorbing or reflecting sun has negligible effect on the solution at 1 AU and beyond [*Englade*, 1971; *Webb and Quenby*, 1973; *Ng and Gleeson*, 1975].

We have found that for the range of parameters used, adequate accuracy can be obtained with 10% spatial steps ($\Delta q = 0.095$) and time steps of 0.2 hour. We did find the numerical solution to be unstable at the near-sun grid points, but this apparently had no effect on the solution beyond about $r = 0.5$ AU (see also *Ng and Gleeson* [1975]). The numerical solution was compared with the available analytic solutions—$b = 0$ with *Lupton and Stone*'s [1973] solution, $b = 1$ and L large with the solution of *Fisk and Axford* [1968], and $V = 0$ with b variable with the solution of *Parker* [1963] for the pure diffusion case—and agreement in all cases was excellent.

Although (2), as written, applies to the case of spherical symmetry with isotropic diffusion, it also describes the situation of anisotropic diffusion ($K_\parallel \gg K_\perp$) within the corotating flux tube from the flare site [*Parker*, 1965; *Ng and Gleeson*, 1971], provided that we identify the radial diffusion coefficient K_r with $K_\parallel \cos^2 \psi$, where ψ is the Archimedean spiral angle.

Simultaneous Observations at Well-Separated Radial Positions

General Comments

Four solar particle events (SPE) will now be discussed individually. These are events during which both earth at 1 AU and Pioneer 10 and/or Pioneer 11 further from the sun were well connected to the flare site (or coronal release site) by the interplanetary magnetic field. Table 3 contains information taken from Solar-Geophysical Data reports concerning the parent solar flares of these particle events as well as others to be discussed in a later section. In all cases the SPE is referred to by the date on which the optical flare occurred. The time of particle injection ($t = 0$ for the numerical solution) was assumed to be the time of the Hα maximum less the 8-min sun-earth light transit time. For flares which occurred beyond the sun's limb the time of X ray or radio burst maximum was used in lieu of Hα observations. The four events discussed in this section all had parent flares on the visible hemisphere of the sun.

The particle intensity-time profiles for these four events are shown in Figures 4–8. Proton fluxes are presented for all four events; however, only for the November 3, 1973, event was it possible to measure also the 1- to 2-MeV electron flux of solar origin at Pioneer 10 or 11. There are two reasons for this. One is that there is a high background of Compton electrons in the 1- to 2-MeV electron channel owing to the intense γ ray flux ($E_\gamma < 2.6$ MeV) from the radioisotope thermoelectric generators (RTG), which supply the electrical power on Pioneer 10 and 11. The second reason is that the flux of MeV electrons of Jovian origin is generally so large beyond about 3½ AU [*Pyle and Simpson*, 1977] that it dominates the solar electron flux for all but the largest flares.

Quiet time background levels have been subtracted from the fluxes shown for both protons and electrons. Fits to the observed profiles using the previously described numerical method are shown as dashed lines superimposed on the data. The intensity normalization has been adjusted individually at each radial distance, so that the shape and time to maximum of the curves can be compared easily with the data. Differences between the theoretically expected radial dependence of intensities and that observed will be discussed later in this section.

Two parameters, K_r(1 AU) and b, were adjusted to obtain agreement with the observed t_m. We chose to fit the observed

TABLE 3. Parent Flare Information

Flare Date	Day of Year	Importance	Location	McMath Region	Time of Hα Maximum	X ray	Sudden Ionospheric Disturbance	Radio Burst Type
June 8, 1972	160	?	~115°W	11895*	1321 (X ray)	yes	no	2
Sept. 6, 1972	250	?	~95°W	12005*	2137 (4)	no	yes	2, 4
Nov. 25, 1972	330	1B	6°S, 44°W	12115	0830	yes	yes	2, 4
Nov. 28, 1972	333	1N	8°S, 80°W	12115	0403	yes	yes	2, 4
Sept. 7, 1973	250	2B	18°S, 46°W	12507	1212	yes	yes	2, 4
Sept. 17, 1973	260	?	~125°W	12513*	1518 (2)	no	no	2
Nov. 3, 1973	307	2N	18°S, 85°W	12584	0034	yes	yes	2, 4
Nov. 5, 1974	309	1N	12°S, 78°W	13310	1538	?	yes	2, 4
July 27, 1975	208	?	~114°E	13786*	1830 (4)	no	no	4

Question marks indicate that no data are available.
*Chosen as most likely candidate because of location and future or previous flare activity.

21562202, 1977, 16, Downloaded from https://agupubs.onlinelibrary.wiley.com/doi/10.1029/JA082i016p02157 by Utah State University, Wiley Online Library on [13/06/2025]. See the Terms and Conditions (https://onlinelibrary.wiley.com/terms-and-conditions) on Wiley Online Library for rules of use; OA articles are governed by the applicable Creative Commons License

t_m rather than to adjust the parameters to obtain a 'good fit' for the whole duration of the event because we felt that t_m can be determined fairly unambiguously, that diffusion primarily determines the profile until maximum intensity, and that corotation effects frequently become a complicating factor during the decay phase, even for prompt events.

The remaining parameters, L, γ, V, were either measured or held constant at reasonable values. The free escape boundary was placed at $L = 20$ AU for consistency with the small radial gradient of galactic cosmic rays found by Pioneer 10 and 11 [*McKibben*, 1975, and references therein] and with the diffusive profiles of SPE's which we and others [*Zwickl et al.*, 1975] have observed at distances of about 5 AU. Placed at this large distance, the outer boundary has no effect on any of the calculated intensity profiles shown, even up to the latest time shown of 14 days after the flare.

The spectral index γ for the protons was measured for each event. Figure 3 presents the differential energy spectrums for the four events to be discussed. One assumption of the model used is that adiabatic deceleration is the only energy change process. If this is the case, a power law energy spectrum should be maintained with no change in slope as a function of radial distance. We see from Figure 3 that the spectral index measured at Pioneer 10 or 11 is indeed almost the same as that measured at earth. Following the argument of *Van Hollebeke et al.* [1975] that an energy spectrum measured near maximum proton intensity is representative of the source spectrum when the observer has good field connection to the flare site, we averaged the spectrum at each radial distance over the time interval during which both the 11- to 20-MeV protons and the 30- to 67-MeV protons reached maximum intensity at that distance. Since maximum intensity of the 11- to 20-MeV protons occurred up to a full day after that of the 30- to 67-MeV protons at several astronomical units, long averages were required to remove the velocity dispersion effect from the measured energy spectrums.

It is not possible to determine experimentally the detailed energy spectrum of the electrons which stop in the second detector of the instruments used (1- to 2-MeV electrons). Therefore a typical value of $\gamma = 3$ [cf. *Simnett*, 1974] was used throughout. The parameter γ in the numerical model is the spectral index for the differential number density. However, we measure the spectral index δ of the omnidirectional differential flux ($dJ/dT \propto T^{-\delta}$). The relation between the two is $dJ/dT = vU/4\pi$, where v is the particle velocity, so $\gamma \simeq \delta + 1$ for the nonrelativistic protons and $\gamma \simeq \delta$ for the electrons, which are relativistic.

The solar wind speed V was taken to be 400 km/s in all the numerical solutions. The measured solar wind speeds at earth and Pioneer 10 and 11 were available and will be used extensively in determining the solar connection longitude of each spacecraft. However, the measured speeds were not utilized in the numerical solution because what is actually needed is the local solar wind speed along the energetic particle path from the sun to the observer. What we have instead is the time history of the solar wind speed at two or three positions in space, and except in certain special cases the information we need does not easily follow from that which we have. Therefore a typical value of 400 km/s was used. The error introduced by this approximation should be of secondary importance.

The validity of our determination of the radial diffusion

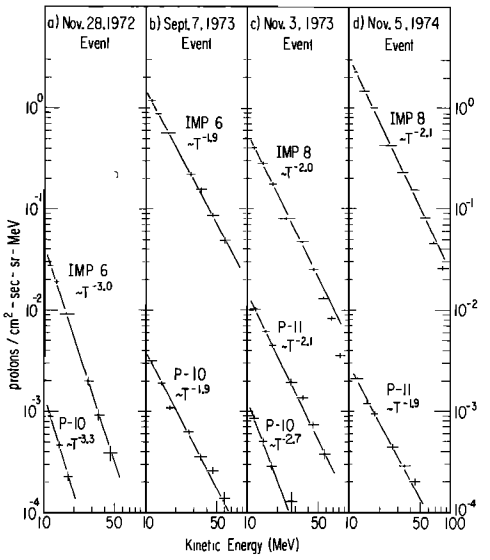

Fig. 3. Energy spectrums of the differential proton flux near the time of maximum intensity for the four solar flare particle events discussed in the text. Power law fits to the spectrums are shown as solid lines. The time intervals included in each spectrum are as follows: (*a*) Imp 6, day 333, 0700–1400; Pioneer 10, day 334, 0000–2400; (*b*) Imp 6, day 250, 1400–2000; Pioneer 10, 0000 hours on day 252 to 0000 hours on day 254; (*c*) Imp 8, day 307, 0400–1000; Pioneer 11, 1800 hours on day 307 to 0600 hours on day 308; Pioneer 10, day 312, 0000–2400; (*d*) Imp 8, day 309, 1800–2400; Pioneer 11, 0000 hours on day 311 to 1200 hours on day 313.

parameters from SPE intensity profiles depends largely on our success in choosing events for which azimuthal propagation effects are of little importance at least until the time of maximum intensity. One method of deciding whether corotation (i.e., convection of a longitudinally confined population of particles) is affecting the particle intensity profile is to calculate the solar connection longitude of the magnetic flux tube containing the observer. A rapidly changing connection longitude implies that the observed intensity profile may be largely due to a passing spatial structure [see *Roelof and Krimigis*, 1973].

To determine those events (and time periods within an event) for which radial propagation primarily determines the intensity profile, we have used the measured solar wind speed to calculate the connection longitude of each spacecraft as a function of time. Following *Nolte and Roelof* [1973], we assume that each plasma element has traveled radially at a constant speed from $r = 0$ and that the magnetic field line at the spacecraft originates at the same solar longitude as the plasma element. Nolte and Roelof estimated that this constant velocity approximation has about 10° accuracy at 1 AU when the solar wind is not evolving rapidly. The accuracy is certainly worse when the extrapolation is made back to the sun from several astronomical units, but the approximation will still be useful for indicating trends and large effects. The constant speed approximation should be most accurate during periods of constant solar wind speed or during the decay portion of fast streams. It should be least accurate at the leading edge of a fast stream, where the fast solar wind is overtaking slower wind and is very likely decelerating.

The instantaneous solar connection longitude in the Carrington system is plotted in the lowest panel of Figures 4, 5, 6, and 8 for each spacecraft using the solar wind speed measured

21562202, 1977, 16, Downloaded from https://agupubs.onlinelibrary.wiley.com/doi/10.1029/JA082i016p02157 by Utah State University, Wiley Online Library on [13/06/2025]. See the Terms and Conditions (https://onlinelibrary.wiley.com/terms-and-conditions) on Wiley Online Library for rules of use; OA articles are governed by the applicable Creative Commons License

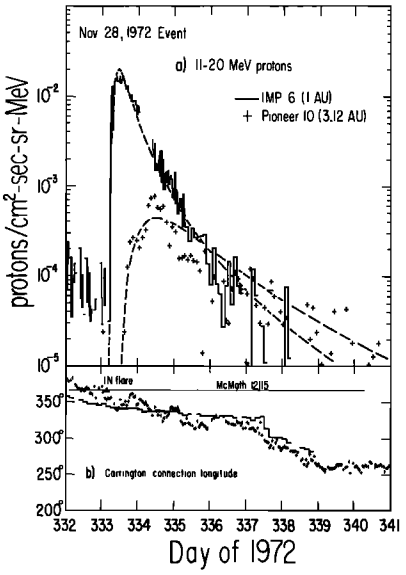

Fig. 4. (*a*) Intensity-time profiles of 11- to 20-MeV protons from the November 28, 1972, solar flare. The dashed lines show model fits with $K_r(1\text{ AU}) = 1.6 \times 10^{21}$ cm²/s, $b = 0.5$, and $\gamma = 3.5$. (*b*) Carrington connection longitude (CCL) of Pioneer 10 (crosses) and earth (solid line). The flare occurred at a Carrington longitude (CL) of 8° in McMath region 12115, and the flare site is shown as a horizontal solid line.

at that spacecraft. The Carrington longitude system is fixed on the surface of the sun and increases westward. The longitude of a sunspot group, for example, remains at a nearly constant Carrington longitude except for small motions of the group with respect to the solar surface. However, the Carrington longitude of the foot of the flux tube which connects a spacecraft to the sun decreases at the Carrington rotation rate (14.2°/d for a spacecraft stationary with respect to the fixed stars, 13.2°/d for an earth satellite) if the solar wind speed is constant. If the solar wind speed is decreasing, the calculated connection longitude will decrease more slowly. At times the decay rate of the solar wind speed is such that the connection point remains at almost the same place on the sun for a period of time. This is known as a 'dwell' period [*Roelof and Krimigis*, 1973].

The solar wind speeds used are 3-hour averages for the near-earth measurement, provided by S. J. Bame and W. C. Feldman, and either 1-hour points or daily snapshots, provided by J. H. Wolfe, for Pioneer 10 and 11. When only daily samples were available, the connection longitude was plotted at midday, but the sample may have been taken at any time during the day. (See *Intriligator* [1974] for estimates of the accuracy of this type of daily snapshot data.)

November 28, 1972, Event (Day 333)

The 11- to 20-MeV proton flux is shown in Figure 4*a*. This relatively small SPE did not produce a measurable enhancement of the 30- to 67-MeV proton flux at Pioneer 10. The solar wind speed at earth steadily decreased from day 332 to day 337, so that earth's Carrington connection longitude (CCL) changed less than 15° in the 4½ days following the flare, as shown in Figure 4*b*. Since the CCL of earth was close to the flare site and was fairly constant in time, one would expect the intensity-time profile observed to reflect propagation of the flare particles along the flux tube, even during the decay phase. So although the best fit values for this event, $b = 0.5$ and $K_r(1\text{ AU}) = 1.6 \times 10^{21}$ cm²/s, were determined from the values of t_m only, the model prediction should agree with the observed profile during the decay phase also if the model is reasonably complete. We note that there is good agreement with the 1-AU profile for several days after the event. The intensity profile at Pioneer 10 is not particularly smooth, but t_m can still be determined with reasonable accuracy.

September 7, 1973, Event (Day 250)

This event (see Figure 5) is complicated by the fact that there was a second injection of protons, possibly accompanying a type 2 radio burst which occurred at 1720 on September 8 (day 251). This second injection produced a population of protons with a much softer energy spectrum than the flare on day 250, as can be seen from the relative intensity of 11- to 20-MeV and 30- to 67-MeV protons at earth. Effects of the second injection are not obvious at Pioneer 10. Imp 6 was in earth's magnetosphere until about 1330 on day 250, so the early part of the onset phase is missing. Figure 5*c* shows that Pioneer 10 was in a solar wind dwell region for this entire period, its CCL remaining nearly constant. Corotation effects should thus be minimized. It is somewhat surprising that even though the CCL of Pioneer 10 is separated by ~130° from the flare site, the flare particles apparently still had rapid access to the Pioneer 10 flux tube.

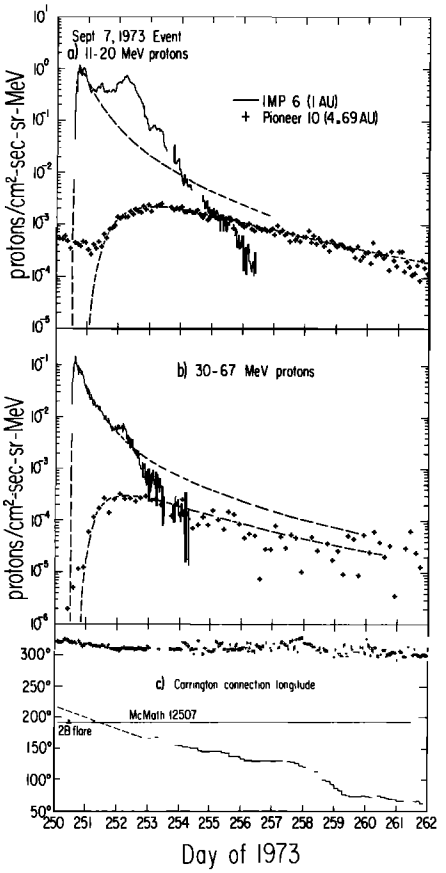

Fig. 5. (*a*) Intensity-time profiles of 11- to 20-MeV protons from the September 7, 1973, solar flare. The dashed lines show model fits with $K_r(1\text{ AU}) = 1.8 \times 10^{21}$ cm²/s, $b = 0.3$, and $\gamma = 2.5$. (*b*) Intensity-time profiles of 30- to 67-MeV protons. The dashed lines show model fits with $K_r(1\text{ AU}) = 3.0 \times 10^{21}$ cm²/s, $b = 0.3$, and $\gamma = 2.5$. (*c*) Carrington connection longitude for Pioneer 10 (crosses) and earth (solid line). The dashed line is a linear interpolation of earth's connection longitude across a 4½-day solar wind data gap from day 248 to day 253. The flare occurred at a CL of 193° in McMath region 12507.

21562202, 1977, 16, Downloaded from https://agupubs.onlinelibrary.wiley.com/doi/10.1029/JA082i016p02157 by Utah State University, Wiley Online Library on [13/06/2025]. See the Terms and Conditions (https://onlinelibrary.wiley.com/terms-and-conditions) on Wiley Online Library for rules of use; OA articles are governed by the applicable Creative Commons License

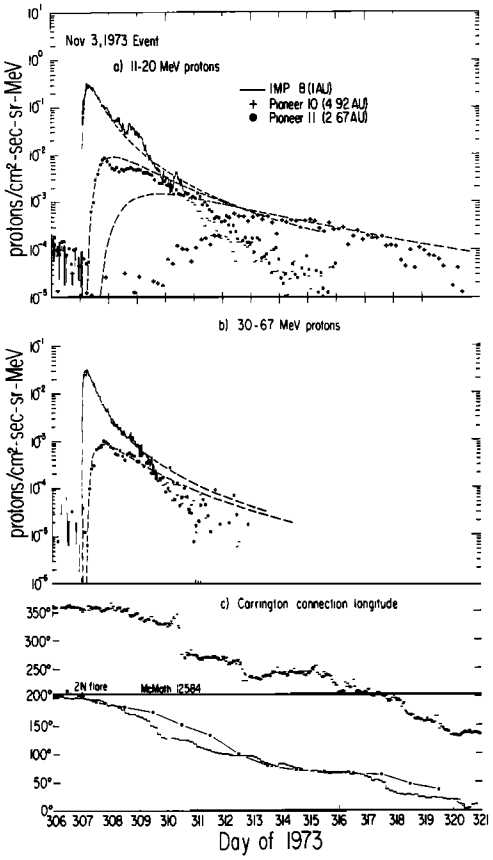

Fig. 6. (*a*) Intensity-time profiles of 11- to 20-MeV protons from the November 3, 1973, solar flare. The dashed lines show model fits with $K_r(1\text{ AU}) = 1.7 \times 10^{21}$ cm²/s, $b = 0.4$, and $\gamma = 2.5$. (*b*) Intensity-time profiles of 30- to 67-MeV protons. The proton flux in this energy range remained near background level at Pioneer 10 and is not shown. The dashed lines show model fits with $K_r(1\text{ AU}) = 2.8 \times 10^{21}$ cm²/s, $b = 0.4$, and $\gamma = 2.5$. (*c*) Carrington connection longitude for Pioneer 10 (crosses), Pioneer 11 (solid circles), and earth (solid line). The flare occurred at a CL of 206° in McMath region 12584.

The intensity profiles at Pioneer 11, which was 2.2 AU from the sun at this time, are very distorted. The maximum intensity of 11- to 20-MeV protons occurred later at Pioneer 11 than at Pioneer 10 even though Pioneer 11 was less than half as far from the sun and was, according to the constant radial velocity approximation, connected to a point closer to the flare site. We are led to conclude that the structure of the coronal magnetic field must have been such that the energetic protons were able to travel easily the large distances in the corona from the flare site to the foot of the Pioneer 10 flux tube but did not have such easy access to the Pioneer 11 flux tube. There is a possibility, of course, that the SPE observed at Pioneer 10 had a different parent flare than the event at earth. The similarity of the energy spectrums at the two positions (see Figure 3) argues against this, however.

The best fit parameters are $b = 0.3$ and $K_r(1\text{ AU}) = 1.8 \times 10^{21}$ cm²/s for the 11- to 20-MeV protons and $K_r(1\text{ AU}) = 3.0 \times 10^{21}$ cm²/s for the 30- to 67-MeV protons. The model curve agrees with the observed 30- to 67-MeV protons at Imp 6 for about 2 days after the flare. The decay was more rapid than predicted thereafter, perhaps owing to corotation effects (see Figure 5*c*). The profile of the 11- to 20-MeV protons is so altered by the second injection of particles that it is not possible to compare it with the model after maximum intensity. There is excellent agreement with the observed 11- to 20-MeV proton flux at Pioneer 10 for 11 days after the flare. Model agreement with the observed 30- to 67-MeV proton flux at Pioneer 10 is also good.

November 3, 1973, Event (Day 307)

There was also a possible second injection of particles during this event (see Figure 6) after the original 2N flare early on day 307. An X ray event peaked at 2001 on day 308, presumably accompanying a flare in McMath region 12584, which had by then rotated beyond the western limb of the sun. This second event did produce prompt electrons (see the second peak in Figure 7), but the secondary increase in the 11- to 20-MeV proton flux seen at Imp 8 on day 308 preceded this flare somewhat and may be due to another event or may be associated with a sector boundary crossing on day 308.

The best fit values for this event are $b = 0.4$ and $K_r(1\text{ AU}) = 1.7 \times 10^{21}$ cm²/s for 11- to 20-MeV protons and $K_r(1\text{ AU}) = 2.8 \times 10^{21}$ cm²/s for 30- to 67-MeV protons and were determined from t_m at Imp 8 and Pioneer 11, ignoring the Pioneer 10 result. At Imp 8 the model profile agrees with the observed proton flux for about 2½ days after the flare. Thereafter the proton flux decreased more rapidly than predicted. From Figure 6*c* we see that the eastward motion of earth's CCL away from the flare site could explain the rapid decay. Agreement between model and observation at Pioneer 11 is satisfactory for almost 4 days after the flare. The 11- to 20-MeV proton profile at Pioneer 11 is somewhat distorted near maximum intensity. This may be connected with sector boundary crossings observed near that time (E. J. Smith, private communication, 1975).

The third dashed line in Figure 6*a* is the predicted profile for 11- to 20-MeV protons at Pioneer 10 (at 4.9 AU) using the values of b and $K_r(1\text{ AU})$ determined from Imp 8 and Pioneer 11. Onset and maximum intensity at Pioneer 10 both occurred much later than predicted. Figure 6*c* shows that Pioneer 10 was poorly connected to the flare site at the time of the flare. A significant flux increase did not begin until the leading edge of a corotating interaction region (CIR) [*Smith and Wolfe*, 1976],

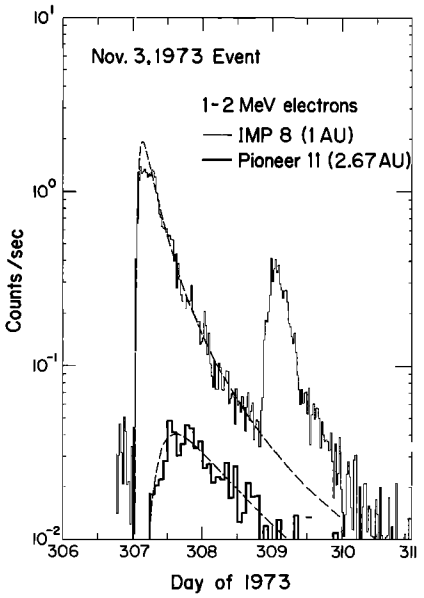

Fig. 7. Intensity-time profiles of 1- to 2-MeV electrons from the November 3, 1973, solar flare. The dashed lines show model fits with $K_r(1\text{ AU}) = 3.7 \times 10^{21}$ cm²/s, $b = 0.4$, and $\gamma = 3.0$.

21562202, 1977, 16, Downloaded from https://agupubs.onlinelibrary.wiley.com/doi/10.1029/JA082i016p02157 by Utah State University, Wiley Online Library on [13/06/2025]. See the Terms and Conditions (https://onlinelibrary.wiley.com/terms-and-conditions) on Wiley Online Library for rules of use; OA articles are governed by the applicable Creative Commons License

seen in Figure 6c as a rapid eastward movement of the Pioneer 10 CCL corresponding to a sudden increase in the solar wind speed, passed Pioneer 10 on day 310 (E. J. Smith and J. H. Wolfe, private communication, 1975). We conjecture that the late arrival of the flare particles is due to the poor field line connection of Pioneer 10 to the flare site early in the event. This interpretation is supported by the fact that the energy spectrum measured at maximum intensity at Pioneer 10 is steeper than that measured at Imp 8 and Pioneer 11 (see Figure 3). Presumably, the intensity of higher-energy protons within the flux tube from the flare site was already decreasing when Pioneer 10 entered it after the passage of the CIR. During the decay phase at Pioneer 10 after day 313 the predicted profile agrees reasonably well with the observed flux.

For this flare it was possible to measure also the 1- to 2-MeV solar electron flux at Pioneer 11. The 1- to 2-MeV electron counting rates at Imp 8 and Pioneer 11 are shown in Figure 7. From the two t_m for the electrons the best fit values are $b = 0.4$ (the same value as that for the protons) and $K_r(1\ \mathrm{AU}) = 3.7 \times 10^{21}$ cm^2/s. So for this event the radial dependence of K_r is independent of particle rigidity from 1 to 400 MV.

November 5, 1974, Event (Day 309)

At Imp 8 the profiles of both the 11- to 20-MeV and the 30- to 67-MeV protons are somewhat distorted near maximum intensity for this event (see Figure 8). There was a sudden flux increase beginning at about 2100 on day 309 which was simultaneous for protons from 1 to 90 MeV. The cause must therefore have been a local feature of the interplanetary medium, although there was no sudden commencement at earth near this time. In Figure 8 we see that the flux of 30- to 67-MeV protons had already reached a maximum before 2100. The 11- to 20-MeV protons had not quite reached maximum intensity, however, which complicates the accurate determination of t_m.

Imp 8 was well connected to the flare site at the time of the flare; however, its connection point moved rapidly eastward thereafter. This could contribute to the observed rapid intensity decay at 1 AU compared with that predicted by the model. It is interesting to note that had we specified $L = 2.8$ AU [cf. *Lupton and Stone*, 1973; *Burlaga*, 1967] instead of $L = 20$ AU, the model curve would have agreed with the observed decay rate. A boundary at 2.8 AU is obviously inconsistent with the diffusive profiles observed at Pioneer 10 and 11 for this same event, however.

Pioneer 11 was in a dwell region from day 309 to day 319 (Figure 8c), and we have another example of the model profile agreeing with the observed 11- to 20-MeV proton flux for 11 days after the flare. The exponential decay rate is matched almost exactly by the model curve. It is important to reiterate that the free escape boundary at 20 AU has no effect on the model curve. The rate of decay here is determined by magnitude and radial dependence of K_r and the effects of convection and adiabatic deceleration.

Figure 8c shows that the CCL of Pioneer 10 was far from the flare site until the same solar wind stream which produced the long dwell at Pioneer 11 reached Pioneer 10 on day 313. Consequently, the onset at Pioneer 10 was later than had been predicted by using the values $b = 0.3$ and $K_r(1\ \mathrm{AU}) = 1.8 \times 10^{21}$ cm^2/s for 11- to 20-MeV protons and $K_r(1\ \mathrm{AU}) = 3.0 \times 10^{21}$ cm^2/s for 30- to 67-MeV protons, which were determined from the Imp 8 and Pioneer 11 profiles. The fit is satisfactory during the decay phase.

Rigidity Dependence of the Mean Free Path

The radial mean free path at 1 AU is related to the radial diffusion coefficient at 1 AU by $\lambda_r(1\ \mathrm{AU}) = 3K_r(1\ \mathrm{AU})/v$, where v is the speed of the particle. Table 4 summarizes the results for the four events discussed previously. The uncertainties will be discussed in the next section.

For some energy intervals of the protons, and for the 1- to 2-MeV electrons for all but the November 3, 1973, event, there was no measurement at Pioneer 10 or 11. For these particles, $K_r(1\ \mathrm{AU})$ was determined from $t_m(1\ \mathrm{AU})$ alone, assuming the value of b to be the same as that for those species for which there were multispacecraft measurements for that event. Figure 9 presents $\lambda_r(1\ \mathrm{AU})$ as a function of particle magnetic rigidity, and we find, as have others [e.g., *Ma Sung et al.*, 1975], that any rigidity dependence from 1 to 400 MV is very weak.

Uncertainty in the Determination of b and $K_r(1\ AU)$

Since we are working with a numerical solution to the transport equation, there is some difficulty in determining the

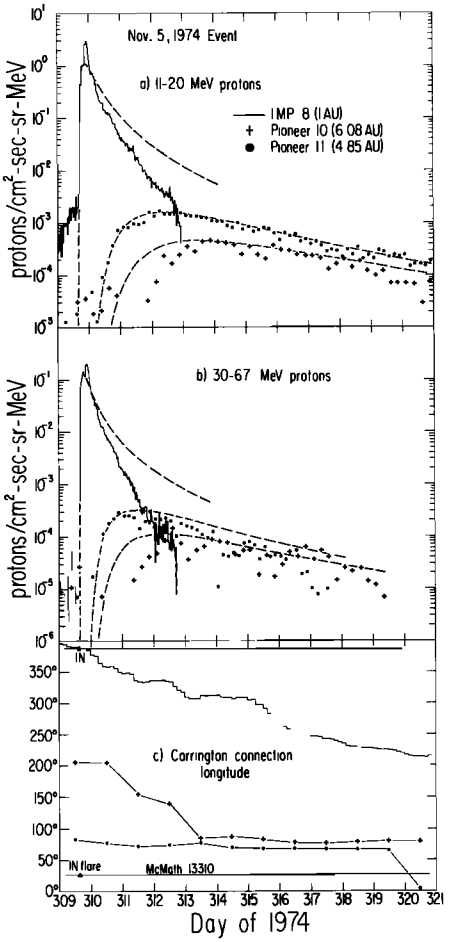

Fig. 8. (*a*) Intensity-time profiles of 11- to 20-MeV protons from the November 5, 1974, solar flare. The dashed lines show model fits with $K_r(1\ \mathrm{AU}) = 1.8 \times 10^{21}$ cm^2/s, $b = 0.3$, and $\gamma = 2.5$. (*b*) Intensity-time profiles of 30- to 67-MeV protons. The dashed lines show model fits with $K_r(1\ \mathrm{AU}) = 3.0 \times 10^{21}$ cm^2/s, $b = 0.3$, and $\gamma = 2.5$. (*c*) Carrington connection longitude for Pioneer 10 (crosses), Pioneer 11 (solid circles), and earth (solid line). The flare occurred at a CL of 27° in McMath region 13310.

21562202, 1977, 16, Downloaded from https://agupubs.onlinelibrary.wiley.com/doi/10.1029/JA082i016p02157 by Utah State University, Wiley Online Library on [13/06/2025]. See the Terms and Conditions (https://onlinelibrary.wiley.com/terms-and-conditions) on Wiley Online Library for rules of use; OA articles are governed by the applicable Creative Commons License

TABLE 4. Summary of Transport Parameters

Solar Particle Event	Species	Energy Range, MeV	t_m(1 AU), hours	b	K_r(1 AU), 10^{21} cm^2/s	λ_r(1 AU), AU
Nov. 28, 1972	proton	11–20	6.6 ± 1.2	0.5 ± 0.2	1.6 ± 0.4	0.063 ± 0.014
	proton	30–67	4.5 ± 1.0	0.5*	2.5 ± 0.6	0.057 ± 0.013
	electron	1–2	2.8 ± 0.4	0.5*	5.0 ± 1.1	0.035 ± 0.008
Sept. 7, 1973	proton	11–20	5.8 ± 1.0	0.3 ± 0.1	1.8 ± 0.3	0.069 ± 0.013
	proton	30–67	3.8 ± 0.4	0.3 ± 0.1	3.0 ± 0.4	0.067 ± 0.009
	electron	1–2	1.4 ± 0.3	0.3*	8.9 ± 1.2	0.062 ± 0.008
Nov. 3, 1973	proton	11–20	6.4 ± 0.6	0.4 ± 0.3	1.7 ± 0.4	0.065 ± 0.014
	proton	20–30	5.2 ± 0.6	0.4*	2.2 ± 0.5	0.064 ± 0.014
	proton	30–67	4.2 ± 0.6	0.4 ± 0.2	2.8 ± 0.6	0.063 ± 0.013
	electron	1–2	3.5 ± 1.0	0.4 ± 0.3	3.7 ± 1.3	0.026 ± 0.009
Nov. 5, 1974	proton	11–20	5.8 ± 0.8	0.3 ± 0.1	1.8 ± 0.3	0.069 ± 0.011
	proton	20–30	4.9 ± 0.8	0.3*	2.2 ± 0.4	0.065 ± 0.011
	proton	30–67	3.8 ± 0.3	0.3 ± 0.2	3.0 ± 0.4	0.067 ± 0.008
	electron	1–2	1.5 ± 0.3	0.3*	8.3 ± 1.0	0.058 ± 0.007

*Same value of b assumed to apply in this energy interval for this event as that for those in which b was determined by multispacecraft observations.

uncertainties which should be assigned to the values we have found for b and K_r(1 AU). However, if the diffusive term dominates in (1), we can make a first-order estimate of Δb and ΔK_r(1 AU) in terms of the Δt_m using standard error analysis and the pure diffusion model for which an analytic solution exists. Then, given Δt_1 and Δt_2, the uncertainties in the time to maximum intensity at r_1 and r_2, we can write

$$\Delta b = \left[\ln\left(\frac{r_1}{r_2}\right)\right]^{-1}\left[\left(\frac{\Delta t_1}{t_1}\right)^2 + \left(\frac{\Delta t_2}{t_2}\right)^2\right]^{1/2}$$

Similarly,

$$\Delta K_r(1\text{ AU}) = K_r(1\text{ AU})\left[\left(\frac{\Delta b}{2-b}\right)^2 + \left(\frac{\Delta t_m(1\text{ AU})}{t_m(1\text{ AU})}\right)^2\right]^{1/2}$$

These expressions should be approximately correct as long as $CVU/[K_r\,(\partial u/\partial r)] \ll 1$, which expresses the requirement that diffusion dominate. If we use the pure diffusion solution to estimate K_r $(\partial u/\partial r)$, we obtain the requirement that $(2 - b)CVt/r \ll 1$. Evaluating this ratio at t_m at the various radial distances, we find that only for the electrons is it less than 0.1. For the protons it varies from ~0.2 at 1 AU to ~0.4 at 5 AU. The effects of convection and deceleration are thus important but not dominant by the time of maximum intensity for protons in the 11- to 67-MeV energy range. So we expect the expressions given above for Δb and ΔK_r(1 AU) to give reasonable but not exact results. They were used to calculate the uncertainties in b and K_r(1 AU) listed in Table 4. The uncertainty in λ_r(1 AU) follows directly from that in K_r(1 AU).

The calculated values of Δb lie between 0.13 and 0.32. As a check that these estimates using the pure diffusion solution are reasonable, we present again, as an example, the 11- to 20-MeV proton profiles from the November 5, 1974, event in Figure 10. The best fit value of b for this event was 0.3. The dashed curves illustrate the change in the predicted profile at 4.85 AU when the best fit value of b is changed by 0.2 (a typical value of Δb) while K_r(1 AU) is simultaneously adjusted to produce the same t_m at 1 AU. We conclude from Figure 10 that t_m at 4.85 AU is fairly certain to lie between those of these two predictions, so that $\Delta b = 0.2$ can be considered a representative uncertainty in b as estimated by using the pure diffusion approximation and also by varying the parameters of the numerical solution.

Radial Variation of Maximum Intensity

As was mentioned earlier, the model curves were adjusted vertically to match the observed maximum flux at each spacecraft for easy comparison of the model to the data. In fact, of course, the model predicts what the relative maximum intensities should be at any two radial distances. We now compare the observations with the predictions.

If the cross section (perpendicular to the radial direction) of the flux tube in which the flare particles are confined increases with r as r^a, then for the case of pure diffusion the maximum intensity should vary as $r^{-(a+1)}$, independent of the value of b [*Parker*, 1963]. Equation (2) assumes that $a = 2$. This is appropriate for diffusion in three-dimensional space from a point source and also for diffusion in a spiral flux tube, assuming a homogenous solar wind speed. When the effects of convection and energy loss are included, U_{max} decreases somewhat more rapidly with r, but for the range of parameters used

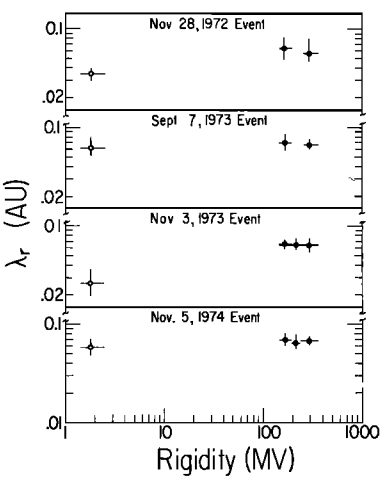

Fig. 9. The rigidity dependence of the radial mean free path at 1 AU for the four solar particle events discussed in the text. Open circles are from measurements of 1- to 2-MeV electrons, and solid circles are from proton measurements.

21562202, 1977, 16, Downloaded from https://agupubs.onlinelibrary.wiley.com/doi/10.1029/JA082i016p02157 by Utah State University, Wiley Online Library on [13/06/2025]. See the Terms and Conditions (https://onlinelibrary.wiley.com/terms-and-conditions) on Wiley Online Library for rules of use; OA articles are governed by the applicable Creative Commons License

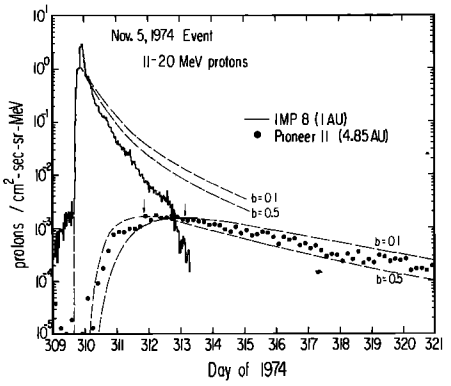

Fig. 10. Illustration of the variations in the model curves when b is changed by 0.2 from its best fit value. $K_r(1\ \mathrm{AU})$ was adjusted to keep t_m at 1 AU constant. The parameters for the two curves are $b = 0.1$, $K_r(1\ \mathrm{AU}) = 1.6 \times 10^{21}\ \mathrm{cm^2/s}$ and $b = 0.5$, $K_r(1\ \mathrm{AU}) = 2.1 \times 10^{21}\ \mathrm{cm^2/s}$. The arrows mark the times of maximum intensity at 4.85 AU predicted by the two curves.

in this paper the dependence is still approximately a power law. For example, for the four events just discussed the model predicts $U_{\max} \propto r^{-3.3}$ to $r^{-3.5}$ for the 11- to 20-MeV protons and $U_{\max} \propto r^{-3.2}$ for the 30- to 67-MeV protons. For the November 28, 1972, and November 3, 1973, events the relative fluxes agree with the model predictions to within about 30%, which is reasonably good considering intercalibration uncertainties among the various instruments used. However, for the September 7, 1973, and November 5, 1974, events the relative flux at Pioneer 10 and 11 (4.7–6.1 AU) was only $\frac{1}{3}$–$\frac{1}{2}$ that predicted. The r dependence between 1 and ~5 AU for these events was approximately $U_{\max} \propto r^{-3.9}$ to $r^{-4.0}$ for the 11- to 20-MeV protons and $U_{\max} \propto r^{-3.8}$ to $r^{-3.9}$ for the 30- to 67-MeV protons.

At least two factors could contribute to the more rapid decline of $U_{\max}$ with r for these events. In both cases, Pioneer 10 and 11 were in dwell regions during the events. It is easily shown that in ideal dwell regions the flux tube cross section increases as r^3 rather than as r^2, which implies, considering only diffusion, that $U_{\max} \propto r^{-4}$. The other effect is that the positive radial gradient in the solar wind speed in a dwell region increases the rate of adiabatic deceleration, which also causes $U_{\max}$ to fall off slightly more rapidly with r. The fact that the two events which were observed in dwell regions did not conform to the model predictions is then not particularly surprising, since two of the assumptions of the model were violated (namely, the assumed geometry and the rate of energy loss).

Time to Maximum Intensity as a Function of Radial Distance

In this section we relax our previous selection criteria to include for discussion those SPE's which were prompt at Pioneer 10 or Pioneer 11, but not at earth, with the purpose of checking a somewhat larger sample of events for consistency with the parameters found previously. We are then able to add five additional events to the original group of four. In Figure 11, t_m is plotted versus radial distance for the nine events, and the data are listed in Table 5.

We lose some of the advantages of simultaneous observations of an individual event, since now temporal variations in K_r and V, as well as variation in the spectral index γ among events, become a factor. We can expect some scatter in the data due to these variations. However, the most important factor in determining t_m for a prompt event for protons at these energies is K_r, and the variation in it for the original four events was not large. So we might expect the overall trend of the data to indicate reasonably well a suitable value for b and $K_r(1\ \mathrm{AU})$.

We can again use the example of pure diffusion to serve as a guide. Then the radial dependence is given by $t_m \propto r^{2-b}$ [*Parker*, 1963], which would give $t_m \propto r^{1.6}$ for $b = 0.4$. When the effects of convection and adiabatic deceleration are included, the slope is decreased somewhat for the same value of b (e.g., from $r^{1.6}$ to $r^{1.5}$ for the parameters used in Figure 11).

There is a certain amount of ambiguity in deciding which SPE's should be included in the group of well-connected (or prompt) events. Some events should obviously not be included because their intensity-time profiles are greatly distorted in some way, possibly being discontinuous owing to local-structure in the interplanetary medium, having rise times which are as long as their decay times, or otherwise having ill-defined t_m. In most cases these are also the events for which a plot of Carrington connection longitude, such as the plots shown previously, also implies poor connection. However, in some cases the calculated CCL of a spacecraft does not accurately indicate how well it is connected to the flare site, which is not too surprising, since we know that the near-sun magnetic field can be very complex and that the constant radial velocity approximation can be considerably in error, especially at large radial distances. An example of this is the September 7, 1973, event for which the calculated Pioneer 10 CCL was about 130° from the flare site, but the event still seemed consistent with the radial propagation model.

For lack of better selection criteria all SPE's for which the CCL of Pioneer 10 or 11 was within 45° of the flare site at the time of maximum intensity, whose intensity profiles were not excessively distorted, and which had reasonably well defined t_m were chosen. To this group were added the September 7,

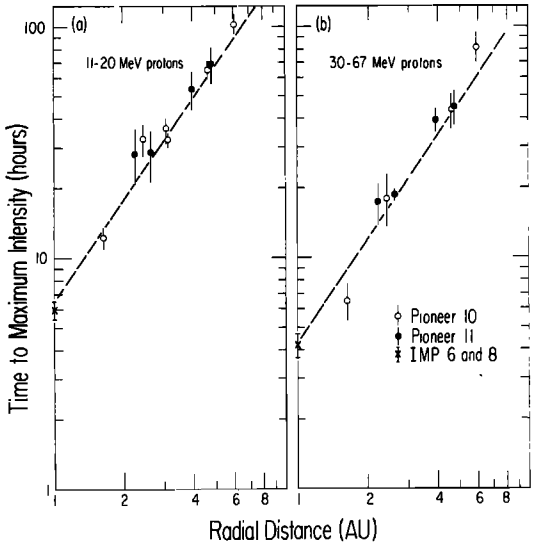

Fig. 11. The radial dependence of the time to maximum intensity for those solar particle events for which connection from the spacecraft to the flare site by the IMF is good. (*a*) Proton energies of 11–20 MeV. The dashed line shows for comparison the model prediction with $K_r(1\ \mathrm{AU}) = 1.7 \times 10^{21}\ \mathrm{cm^2/s}$, $b = 0.4$, $\gamma = 2.5$, $V = 400$ km/s, $L = 20$ AU, and $\alpha = 2$. (*b*) Proton energies of 30–67 MeV. The dashed line shows the model prediction with $K_r(1\ \mathrm{AU}) = 2.8 \times 10^{21}\ \mathrm{cm^2/s}$, $b = 0.4$, $\gamma = 2.5$, $V = 400$ km/s, $L = 20$ AU, and $\alpha = 2$.

21562202, 1977, 16, Downloaded from https://agupubs.onlinelibrary.wiley.com/doi/10.1029/JA082i016p02157 by Utah State University, Wiley Online Library on [13/06/2025]. See the Terms and Conditions (https://onlinelibrary.wiley.com/terms-and-conditions) on Wiley Online Library for rules of use; OA articles are governed by the applicable Creative Commons License

TABLE 5. Times to Maximum Proton Intensity for Prompt Events

	Pioneer 10			Pioneer 11		
		t_m, hours			t_m, hours	
Event Date	r, AU	11–20 MeV	30–67 MeV	r, AU	11–20 MeV	30–67 MeV
June 8, 1972	1.66	12.5 ± 1.0	6.3 ± 1.5	···	···	···
Sept. 6, 1972	2.47	34 ± 4	18 ± 5	···	···	···
Nov. 25, 1972	3.10	36 ± 4	···	···	···	···
Nov. 28, 1972	3.12	32 ± 3	···	···	···	···
Sept. 7, 1973	4.69	66 ± 6	43 ± 7	···	···	···
Sept. 17, 1973	···	···	···	2.27	29 ± 8	17 ± 4
Nov. 3, 1973	···	···	···	2.67	27 ± 7	19 ± 3
Nov. 5, 1974	6.08	104 ± 12	79 ± 12	4.85	68 ± 12	44 ± 8
July 27, 1975	···	···	···	4.02	54 ± 10	39 ± 4

1973, event, which was discussed before, the November 5, 1974, event, for which the CCL of both Pioneer 10 and Pioneer 11 were slightly more than 45° from the flare site, and the July 27, 1975, event, for which there was no solar wind speed measurement at Pioneer 11.

A typical value of time to maximum intensity at 1 AU was determined by averaging the Imp 6 and 8 results for six SPE's in 1972, 1973, and 1974 for which the calculated CCL of earth was within 20° of the flare site. The values obtained were 6.1 ± 0.5 hours for 11- to 20-MeV protons and 4.2 ± 0.5 hours for 30- to 67-MeV protons. This is consistent with the result of *Van Hollebeke et al.* [1975], who found a median value of t_m = 4.5 hours for 20- to 80-MeV protons for a large sample of 32 events for which the parent flare was between 20° and 80°W.

For comparison purposes the r dependence predicted by the model with $b = 0.4$, $\gamma = 2.5$, and $V = 400$ km/s is shown as a dashed line in Figure 11. There was no attempt to find the 'best fit' for these data because of the previously discussed variable conditions from event to event. The trend of the data, however, is apparently well represented by the assumed model. The dashed lines form lower bounds on the t_m versus r plots. If the t_m for the other excluded ('nonprompt') events were plotted, they would all lie above those shown.

Discussion and Summary

We have tested the applicability of the standard transport theory including the effects of diffusion, convection, and adiabatic deceleration for describing the radial transport of solar flare particles (proton energy of 11–67 MeV and electron energy of ~1–2 MeV) with the assumption of a power law dependence of K_r on r. When the connection longitude of the observer is close to the coronal release site and is constant during an event, we find no discrepancy between the observed and the theoretically predicted intensity-time profiles during any part, including the decay phase, of the event. We have purposely selected events for analysis for which azimuthal propagation is not an important factor.

We found a radial mean free path at 1 AU of λ_r(1 AU) = 0.065 ± 0.010 AU for protons from 11 to 67 MeV and λ_r(1 AU) = 0.03–0.06 AU for 1- to 2-MeV electrons. The average value of the radial index was $b = 0.4 \pm 0.2$. The rigidity dependence of both λ_r(1 AU) and b was found to be very weak over the range 1–400 MV. As a measure of the importance of including the effects of convection and adiabatic deceleration in the propagation model, we note that if the events had been analyzed in terms of the pure diffusion model, the value of b deduced would be about 0.1 larger and K_r(1 AU) would be from 15 to 40% larger. Furthermore, the predicted decay rates would be considerably slower, which would be in worse agreement with the data.

We have observed that the maximum intensity of an SPE decreases with radial distance as $U_{max} \propto r^{-3}$ to r^{-4}. The observed radial dependence is close to that predicted by the numerical model except in dwell regions. The more rapid radial decline in dwell regions may be attributable to the fact that spatial divergence is rapid there ($a > 2$ where the flux tube cross section varies as r^a) and the rate of adiabatic deceleration is enhanced.

We have found that the outer boundary L of the diffusing region must be beyond 10 AU, which is consistent with the small radial gradient of galactic cosmic ray intensity found by Pioneer 10 and 11 experimenters. The magnitude that we found for K_r is in agreement with the value for 30- to 67-MeV protons reported by *McKibben et al.* [1975], $K_r \sim 2\text{–}3 \times 10^{21}$ cm²/s, which they deduced from the magnitude of the cosmic ray radial gradient. Our value for K_r(1 AU) tends to be larger than values deduced from measurements of the power spectrum of IMF fluctuations and application of quasi-linear theory [e.g., *Jokipii and Coleman*, 1968; *Hedgecock*, 1975]. However, *Sari* [1975] considered separately the power between directional discontinuities in the field and that contributed by the discontinuities. He found the daily variations in the 60- to 80-MeV proton flux to be well correlated with the value of V/K_r when he calculated K_r from the power between discontinuities. The average value he deduced for K_r from the 'between' power implies a mean free path very nearly equal to the one we deduced for protons from 11 to 67 MeV.

It is important to keep in mind that the intensity-time profile of a prompt solar particle event depends on the magnitude of K_r along the whole path from the sun to the point of observation and beyond during the decay phase; i.e., it is an integral effect. So when we assume that $K_r \propto r^b$ for all r, the value of b deduced from SPE t_m measurements is some sort of average value. There is no a priori reason to believe that the radial dependence should be well described by a power law or that the dependence does not change with r. In particular, recent theoretical work by *Skadron and Hollweg* [1976] indicates that we might expect K_r to have a minimum value somewhere between $\frac{1}{3}$ and 1 AU, increasing at both smaller and larger r. However, the fact that we obtained a reasonably consistent value for b for all the events studied indicates that the radial dependence is not changing rapidly between 1 and 5 AU. We hesitate to extrapolate our results beyond the range of r over which the measurements were made. The only indication that $b \sim 0.4$ beyond 5 or 6 AU comes from the agreement of the model prediction with the decay phases of the September 7,

21562202, 1977, 16, Downloaded from https://agupubs.onlinelibrary.wiley.com/doi/10.1029/JA082i016p02157 by Utah State University, Wiley Online Library on [13/06/2025]. See the Terms and Conditions (https://onlinelibrary.wiley.com/terms-and-conditions) on Wiley Online Library for rules of use; OA articles are governed by the applicable Creative Commons License

1973, and November 5, 1974, events observed at almost 5 AU. As more data become available over an even larger range of radial distance, it may be necessary to reexamine the assumption of a power law dependence.

Our result for the radial dependence of the effective radial diffusion coefficient does not specify directly how $K_\parallel$ and $K_\perp$ vary with r. Since $K_r = K_\parallel \cos^2\psi + K_\perp \sin^2\psi$, both $K_\parallel$ and $K_\perp$ can contribute to K_r, and at large r the $K_\perp$ term is weighted much more heavily because ψ approaches 90°. It is probably not a coincidence that the SPE's which appeared prompt at the largest radial distances (September 7, 1973, and November 5, 1974, events) were observed in rarefaction regions (or dwell regions), the declining speed portion of fast solar wind streams [see *Barouch and Burlaga,* 1976]. These are regions of reduced magnetic field strength and are also regions in which the field direction is most widely distributed about the average Archimedean spiral direction (E. J. Smith, private communication, 1976). It is possible that the effect of field line meandering [*Jokipii and Parker,* 1969; *Jokipii,* 1973*a*], which broadens the distribution of particles about the average field direction and thus contributes to the effective $K_\perp$, makes a contribution to radial transport at several astronomical units and beyond, although near earth the mechanism has not been found to be particularly effective [e.g., *Roelof and Krimigis,* 1973].

Conlon [1977], however, has recently found a value of $K_\perp \sim 5 \times 10^{20}$ cm²/s in rarefaction regions near 5 AU from the study of the transport of Jovian electrons (3–6 MeV) across the average IMF. He found $K_\perp$ to be much smaller than this in CIR's and in regions of constant solar wind speed. This value of $K_\perp$ is small in comparison with the value of K_r which we have found, so $K_\parallel$ is probably still the dominant factor even at 5 AU. In this case, $K_r \propto r^{0.4}$ would require $K_\parallel \propto r^{2.4}$ at large r.

Even if we have almost totally anisotropic diffusion ($K_\parallel \gg K_\perp$), it is possible that the r dependence of K_r is different in regions of constant solar wind speed, for example, than in rarefaction regions. The difference in Alfven wave refraction in rarefaction regions, as discussed by *Skadron and Hollweg* [1976], would be one cause. In this case we might expect a solar cycle dependence in the average value of b, since solar wind stream structure seems to have a solar cycle dependence [*Gosling et al.,* 1976]. Our observations were made in 1972–1975, the declining phase of the solar cycle.

There have been a few theoretical investigations of the expected radial dependence of K_r in simplified cases. *Jokipii* [1973*b*] considered two cases. In the first he assumed the particle scattering to be caused by frozen-in magnetic fluctuations. He found $K_r \propto r^{-1}$ asympotically for large r in this case. In the second he assumed the scattering to be due to Alfven waves generated near the sun which propagate outward with wave vectors parallel to the average field direction. In this case he found $K_r \propto r^0$ at large r.

Völk et al. [1974] also considered a model in which all the scattering is due to Alfven waves. They also used the WKB approximation, which neglects any generation or dissipation of the waves in interplanetary space. They found that the wave vectors should refract toward the radial direction as they propagate outward from the sun, so that beyond about 1 AU they would almost all be nearly radial. This results in a much faster radial increase in K_r ($K_r \propto r^3$ at large r and at low heliographic latitudes) than that found by Jokipii. This is due to the fact that the wave vectors are nearly normal to the average field direction at large r, which implies that the waves are very inefficient at scattering charged particles which propagate along the field direction. In both these studies the r dependence of K_r was deduced from that of $K_\parallel$ by using the relation $K_r = K_\parallel \cos^2\psi$. Perpendicular diffusion was neglected.

Two recent papers have again considered the case of scattering due only to Alfven waves but have taken into account additional effects which make the model more realistic. *Skadron and Hollweg* [1976] considered the effect of a nonazimuthally symmetric solar wind on the refraction of the Alfven wave vectors. They used a simplified stream model and found that the wave vectors lie closer to the Archimedean spiral direction in rarefaction regions than they would in an azimuthally symmetric wind. This results in a K_r which increases more slowly with r than the r^3 dependence found by Völk et al. The exact form of the r dependence depends on their assumptions concerning the IMF irregularity power spectrum and also on their stream model. In particular, they found a minimum in K_r at about ⅓–1 AU from the sun. Their K_r for 10-MeV protons increases from 1 to 5 AU with an average value of b less than 1, although the r dependence is not very well represented by a power law over that range.

Morfill et al. [1976] did not consider stream structure but rather considered the effect of medium-scale variations of the IMF direction. This effect reduces the diffusion coefficient at large r where the average IMF is nearly azimuthal, and the Alfven wave vectors are nearly radial because of refraction. Because of the distribution of IMF directions about the average Archimedean spiral direction the wave vectors are sometimes more field aligned and thus are more effective at scattering charged particles. They found K_r to increase out to ~2 AU and to be nearly constant beyond.

Theoretical calculations of the radial variation of K_r are gaining sophistication. They will certainly benefit from refinements of the theory relating the observed power spectrum of IMF fluctuations to particle propagation parameters. Also, further measurements of the power spectrum as a function of heliocentric distance will reduce the need for idealizations in the models.

As for energetic charged particle measurements, additional SPE observations beyond 5 AU and well inside 1 AU, preferably with simultaneous observations at another radial distance, will be useful. Solar cycle effects may become obvious from observations during the increasing phase of the next solar cycle. SPE observations far out of the ecliptic plane will be useful to look for latitude-dependent propagation effects [see *Fisk,* 1976].

After submitting this paper, I have become aware of a preprint by R. D. Zwickl and W. R. Webber (1976) in which they have also deduced the radial dependence of K_r from SPE's but have used a different approach. They report a value of $b = 0.0 \pm 0.3$.

Acknowledgments. I would first of all like to thank my thesis advisor, J. A. Simpson, for his continued support and guidance. The University of Chicago charged particle instruments on Pioneer 10 and 11 and Imp 6 and 8 were designed and constructed by the staff of the Laboratory for Astrophysics and Space Research of the Enrico Fermi Institute under the direction of J. A. Simpson, and the excellence of their work is gratefully acknowledged. K. R. Pyle and C. W. Barnes wrote computer programs which have greatly facilitated this work. I would like to thank G. M. Mason and W. F. Dietrich for their assistance in the use and interpretation of the data from Imp 8 and Imp 6. I have benefited from many stimulating discussions with T. F. Conlon. The generous and timely provision of solar wind data from Pioneer 10 and 11 by J. H. Wolfe of the Ames Research Center and from Imp and Vela satellites by S. J. Bame and W. C. Feldman of the Los Alamos Scientific Laboratory has been extremely helpful. Pioneer 10 and 11 IMF data provided by E. J. Smith of the Jet Propulsion Laboratory have also been very useful. The support provided by the

21562202, 1977, 16, Downloaded from https://agupubs.onlinelibrary.wiley.com/doi/10.1029/JA082i016p02157 by Utah State University, Wiley Online Library on [13/06/2025]. See the Terms and Conditions (https://onlinelibrary.wiley.com/terms-and-conditions) on Wiley Online Library for rules of use; OA articles are governed by the applicable Creative Commons License

Ames Pioneer project office, and in particular by C. F. Hall, A. J. Wilhelmi, and J. E. Lepetich, is much appreciated. This work was supported by NASA under contract NAS 2-6551 and by the National Science Foundation under grant DES 75-20407. This paper was a thesis submitted to the Department of Physics, University of Chicago, in partial fulfillment of the requirements for the Ph.D. degree.

The Editor thanks J. Sari for his assistance in evaluating this paper.

REFERENCES

Barouch, E., and L. F. Burlaga, Three-dimensional interplanetary stream magnetism and energetic particle motion, *J. Geophys. Res., 81,* 2103, 1976.

Burlaga, L. F., Anisotropic diffusion of solar cosmic rays, *J. Geophys. Res., 72,* 4449, 1967.

Conlon, T. F., The interplanetary modulation and transport of Jovian electrons, submitted to *J. Geophys. Res.*, 1977.

Countee, C. R., and L. J. Lanzerotti, Observations and analysis of low-energy solar particle propagation from discrete flare events, *J. Geophys. Res., 81,* 441, 1976.

Cummings, A. C., E. C. Stone, and R. E. Vogt, Interplanetary diffusion coefficients for cosmic rays, *Proc. Int. Conf. Cosmic Rays 13th, 2,* 772, 1973.

Englade, R. C., Effects of the solar boundary condition on flare particle propagation, *J. Geophys. Res., 76,* 6190, 1971.

Feit, J., Confinement of solar flare cosmic rays to sectors of the corotating solar magnetic field, *J. Geophys. Res., 74,* 5579, 1969.

Fisk, L. A., Solar modulation of galactic cosmic rays, 4, Latitude-dependent modulation, *J. Geophys. Res., 81,* 4646, 1976.

Fisk, L. A., and W. I. Axford, Effects of energy changes on solar cosmic rays, *J. Geophys. Res., 73,* 4396, 1968.

Gosling, J. T., J. R. Asbridge, S. J. Bame, and W. C. Feldman, Solar wind speed variations: 1962–1974, *J. Geophys. Res., 81,* 5061, 1976.

Hamilton, D. C., Solar flare proton and electron propagation at large radial distances from the sun (abstract), *Eos Trans. AGU, 56,* 419, 1975.

Hedgecock, P. C., Measurements of the interplanetary magnetic field in relation to the modulation of cosmic rays, *Solar Phys., 42,* 497, 1975.

Hofmann, D. J., and J. R. Winckler, Simultaneous balloon observations at Fort Churchill and Minneapolis during the solar cosmic ray events of July 1961, *J. Geophys. Res., 68,* 2067, 1963.

Intriligator, D. S., The reliability of the daily quick look solar wind velocities as indicators of interplanetary activity, *J. Geophys. Res., 79,* 2491, 1974.

Jokipii, J. R., Propagation of cosmic rays in the solar wind, *Rev. Geophys. Space Phys., 9,* 27, 1971.

Jokipii, J. R., The rate of separation of magnetic lines of force in a random magnetic field, *Astrophys. J., 183,* 1029, 1973*a*.

Jokipii, J. R., Radial variation of magnetic fluctuations and the cosmic-ray diffusion tensor in the solar wind, *Astrophys. J., 182,* 585, 1973*b*.

Jokipii, J. R., and P. J. Coleman, Jr., Cosmic ray diffusion tensor and its variation observed with Mariner 4, *J. Geophys. Res., 73,* 5495, 1968.

Jokipii, J. R., and E. N. Parker, Stochastic aspects of magnetic lines of force with application to cosmic ray propagation, *Astrophys. J., 155,* 777, 1969.

Krimigis, S. M., Interplanetary diffusion model for the time behavior of intensity in a solar cosmic ray event, *J. Geophys. Res., 70,* 2943, 1965.

Lupton, J. E., and E. C. Stone, Solar flare particle propagation: Comparison of a new analytic solution with spacecraft measurements, *J. Geophys. Res., 78,* 1007, 1973.

Ma Sung, L. S., M. A. Van Hollebeke, and F. B. McDonald, Propagation characteristics of solar flare particles, *Proc. Int. Conf. Cosmic Rays 14th, 5,* 1767, 1975.

McCarthy, J., and J. J. O'Gallagher, The radial variation of solar flare proton anisotropies observed in deep space on Pioneers 10 and 11, *Geophys. Res. Lett., 3,* 53, 1976.

McKibben, R. B., Cosmic ray intensity gradients in the solar system, *Rev. Geophys. Space Phys., 13,* 1088, 1975.

McKibben, R. B., K. R. Pyle, J. A. Simpson, A. J. Tuzzolino, and J. J. O'Gallagher, Cosmic ray radial intensity gradients measured by Pioneer 10 and 11, *Proc. Int. Conf. Cosmic Rays 14th, 4,* 1512, 1975.

Meyer, P., E. N. Parker, and J. A. Simpson, Solar cosmic rays of February, 1956 and their propagation through interplanetary space, *Phys. Rev., 104,* 768, 1956.

Morfill, G. E., H. J. Völk, and M. A. Lee, On the effect of directional medium-scale interplanetary variations on the diffusion of galactic cosmic rays and their solar cycle variation, *J. Geophys. Res., 81,* 5841, 1976.

Ng, C. K., and L. J. Gleeson, The propagation of solar cosmic ray bursts, *Solar Phys., 20,* 166, 1971.

Ng, C. K., and L. J. Gleeson, Propagation of solar-flare cosmic rays along corotating interplanetary flux-tubes, *Solar Phys., 43,* 475, 1975.

Nolte, J. T., and E. C. Roelof, Large-scale structure of the interplanetary medium, 1, High coronal source longitude of the quiet-time solar wind, *Solar Phys., 33,* 241, 1973.

Parker, E. N., *Interplanetary Dynamical Processes,* Interscience, New York, 1963.

Parker, E. N., The passage of energetic charged particles through interplanetary space, *Planet. Space Sci., 13,* 9, 1965.

Pyle, K. R., and J. A. Simpson, The Jovian relativistic electron distribution in interplanetary space from 1–11 AU: Evidence for a continuously emitting 'point' source, *Astrophys. J.*, in press, 1977.

Roelof, E. C., and S. M. Krimigis, Analysis and synthesis of coronal and interplanetary energetic particle, plasma, and magnetic field observations over three solar rotations, *J. Geophys. Res., 78,* 5375, 1973.

Sari, J. W., Cosmic ray diffusion tensor and its radial gradient near 1 AU, *Proc. Int. Conf. Cosmic Rays 13th, 2,* 675, 1973.

Sari, J. W., Modulation of low-energy cosmic rays, *J. Geophys. Res., 80,* 457, 1975.

Simnett, G. M., Relativistic electron events in interplanetary space, *Space Sci. Rev., 16,* 257, 1974.

Skadron, G., and J. V. Hollweg, Fokker-Planck theory for cosmic ray diffusion in the presence of Alfvén waves, 2, Model stream calculation, *J. Geophys. Res., 81,* 5887, 1976.

Smith, E. J., and J. H. Wolfe, Observations of interaction regions and corotating shocks between one and five AU: Pioneers 10 and 11, *Geophys. Res. Lett., 3,* 137, 1976.

Van Hollebeke, M. A. I., L. S. Ma Sung, and F. B. McDonald, The variation of solar proton energy spectra and size distribution with heliolongitude, *Solar Phys., 41,* 189, 1975.

Völk, H. J., Cosmic ray propagation in interplanetary space, *Rev. Geophys. Space Phys., 13,* 547, 1975.

Völk, H. J., G. Morfill, W. Alpers, and M. A. Lee, Spatial dependence of the pitch-angle and associated spatial diffusion coefficients for cosmic rays in interplanetary space, *Astrophys. Space Sci., 26,* 403, 1974.

Webb, S., and J. J. Quenby, Numerical studies of the transport of solar protons in interplanetary space, *Planet. Space Sci., 21,* 23, 1973.

Webb, S., A. Balogh, J. J. Quenby, and J. F. Sear, A comparison of theoretical and experimental estimates of the solar proton diffusion coefficient during three flare events, *Solar Phys., 29,* 477, 1973.

Zwickl, R., W. R. Webber, F. B. McDonald, B. Teegarden, and J. Trainor, Solar cosmic ray events at large radial distances from the sun, *Proc. Int. Conf. Cosmic Rays 14th, 12,* 4239, 1975.

(Received October 18, 1976;
accepted February 22, 1977.)

21562202, 1977, 16, Downloaded from https://agupubs.onlinelibrary.wiley.com/doi/10.1029/JA082i016p02157 by Utah State University, Wiley Online Library on [13/06/2025]. See the Terms and Conditions (https://onlinelibrary.wiley.com/terms-and-conditions) on Wiley Online Library for rules of use; OA articles are governed by the applicable Creative Commons License